

Tensor polarization and the dissipative damping of vector meson in QCD Medium

Feng Li^{1,2,3,*} and Shuai Y.F. Liu^{1,2,4,†}

¹*School of Physics and Electronics, Hunan University, Changsha 410082, China*

²*Hunan Provincial Key Laboratory of High-Energy Scale Physics and Applications, Hunan University, Changsha 410082, China*

³*School of Physical Science and Technology, Lanzhou University, Lanzhou 730000, China*

⁴*Quark Matter Research Center, Institute of Modern Physics,
Chinese Academy of Sciences, Lanzhou 730000, China*

(Dated: February 4, 2025)

Unexpectedly large and puzzling spin alignment, and thus tensor polarization, of vector mesons has been observed in heavy-ion collisions. Given that tensor polarization represents a fluctuation of spin, we derive, for the first time, a fluctuation-dissipation relation for tensor polarization, where the polarization is proportional to first-order hydrodynamic gradients (e.g., the shear-stress tensor), with dissipative coefficients depending on the particle's damping properties, as characterized by its spectral function. Phenomenologically, we find that the dissipative contributions have the potential to generate substantial spin alignment and give rise to complex behaviors, providing insights that may help explain the puzzling phenomena observed in experiments.

Introduction.— Spin has played a central role in advancing our understanding of the microscopic quantum world since its discovery. Due to its quantum nature, the measurement of spin is inherently non-deterministic, and we only obtain statistical distributions. Therefore, statistical quantities such as the mean value of the spin vector $\langle S_i \rangle$ (with $i = x, y, z$) and spin fluctuations $\langle S_i S_j \rangle$ are essential for characterizing a particle's spin properties. For spin-1/2 particles, the mean value of the spin vector $\langle S_i \rangle$ is sufficient to determine the complete spin information, i.e., the spin density matrix, of the particle. However, for spin-1 particles, in addition to the vector spin, the symmetric and traceless part of the fluctuation tensor $\langle S_i S_j \rangle$, specifically $\langle S_i S_j - \mathbf{S}^2/3 \rangle$, carries an additional 5 degrees of freedom to characterize the spin density matrix. This quantity, with proper normalization, is referred to as the tensor polarization of spin-1 particles, and has been investigated in many fields in physics [1–8].

In heavy-ion collisions, besides the widely studied vector polarization in experiments [9–13] and theory [14–26], the tensor polarization, related to spin fluctuations, of vector mesons has also been proposed to be an observable [27]. More concretely, the proposed observable is called spin alignment, which refers to the deviation of the “00” component of the spin density matrix from its equilibrium limit: $\delta\rho_{00} = \rho_{00} - 1/3$. This quantity is directly proportional to the zz -component of the tensor polarization: $\delta\rho_{00} \propto \langle 2S_z^2 - S_x^2 - S_y^2 \rangle/3 = T_{zz}$ (quantize along \hat{z}), characterizing how fluctuations in the system are unevenly distributed between the transverse $x - y$ plane and the longitudinal z -direction. However, recent measurements in experiments [28–32] have discovered that the value of the spin alignment is orders of magnitude larger than typical theoretical expectations [33–36], accompanied by puzzling behaviors.

Efforts have also been made from various perspectives [37–41] to understand this puzzle. However, the origin of this unexpected spin alignment remains an

open question [36]. These studies have primarily established non-dissipative relations between spin alignment and other quantities, such as vorticity [33–36] or strong electromagnetic fields [37, 40, 41], with the latter being proposed as an explanation in experimental studies [28]. However, following Einstein's discovery of the physics of Brownian motion, it is understood that the fluctuation of quantities can be naturally linked to dissipative processes. Given that spin alignment represents an anisotropic fluctuation of spin, it is natural to ask whether a fluctuation-dissipation relation can be established in this context—a question that has yet to be explored in the study of spin alignment. Therefore, in this work, we present two key findings from our investigation: (1) Theoretically, we establish, for the first time, a fluctuation-dissipation relation for tensor polarization, where novel dissipative contributions are discovered. (2) Phenomenologically, the new dissipative effects exhibit promising features that shed light on this puzzling spin alignment observed in experiments.

Fluctuation-dissipation relation. — To further illustrate the fluctuation nature of the tensor polarization and spin alignment, we begin with a simplified example of the spin density matrix $\rho_{ss'}$ (or ρ) in the particle's rest frame, where the tensor polarization density T_{ij} can be expressed in terms of the standard 3×3 spin operators S^i (standard representation [42]) as $T_{ij} \propto -\text{Tr}\{\rho(S_i S_j - \mathbf{S}^2/3)\}3n$. Correspondingly, the spin alignment can be expressed as $\delta\rho_{00} \propto T^{zz} \propto \text{Tr}\{\rho(S_x^2 + S_y^2 - 2S_z^2)/3\}$. As shown, both $T_{\mu\nu}$ and $\delta\rho_{00}$ can be interpreted as the fluctuation of spin.

To obtain useful formulations for these quantities, the theory is developed in the following context: vector mesons with momentum $\tilde{p}^\mu = (\varepsilon_{\mathbf{p}}, \mathbf{p})$ at density $n(\varepsilon_u)$ propagate in a locally equilibrated hydrodynamic medium, where their tensor polarization $\mathcal{T}^{\mu\nu}$ can be characterized by hydrodynamic variables such as inverse temperature $\beta = 1/T$, the flow velocity $u^\mu(x)$, symmetric

flow gradients $\xi_{\lambda\gamma} \equiv \beta^{-1}\partial_{(\lambda}(\beta u)_{\gamma)}$, etc. To study general polarization phenomena in this context, we have developed a comprehensive theoretical framework “Zubarev response approach”, which is detailed in “supplementary materials” and in our long theory paper [42]. Especially, in the long paper, we illustrate how our “Zubarev response approach”, rooted rigorously in thermal field theory, can systematically calculate various polarization phenomena, including the dissipative and non-dissipative contribution on equal footing, and lay out the path to incorporating non-perturbative methods, such as lattice methods and the functional renormalization group.

There are many new dissipative and non-dissipative effects predicted by the “Zubarev response approach” to the spin alignment problem, where the fluctuation and dissipation relation are naturally encoded. In this letter, we will focus on discussing one of the main discoveries—shear-induced tensor polarization effects (SITP), using it as an example to highlight how dissipative contributions, overlooked by the community for decades, can impact the phenomenology of spin alignment physics. Using SITP effect as an example, the uneven spin fluctuation characterized by tensor polarization $\mathcal{T}^{\mu\nu}$ can be expressed as

$$\mathcal{T}^{\mu\nu} = \tilde{\Delta}_\lambda^{(\mu} \tilde{\Delta}_\gamma^{\nu)} [\beta n(\varepsilon_u) \alpha_{\text{sh}} \xi^{\gamma\lambda}] \quad (1)$$

which naturally relates to the dissipative processes in-medium through a T-odd dissipative coefficient as

$$\begin{aligned} \alpha_{\text{sh}} &= \frac{4\varepsilon_{\mathbf{p}}\pi}{\beta n(\varepsilon_{\mathbf{p}})} \int_0^\infty d\omega \frac{\partial n(\omega)}{\partial \omega} (\omega^2 - \varepsilon_{\mathbf{p}}^2) A^2(\omega, \mathbf{p}) \\ &\approx -\frac{2\Delta\varepsilon_{\mathbf{p}}}{\Gamma_{\mathbf{p}}} + 2\frac{\Delta\varepsilon_{\mathbf{p}}}{\Gamma_{\mathbf{p}}} \frac{\Delta\varepsilon_{\mathbf{p}}}{T} + \frac{\Gamma_{\mathbf{p}}}{2T}, \end{aligned} \quad (2)$$

where the spectral function $A(\omega, \mathbf{p})$ controls the dissipative damping of a particle’s propagation as $D(t, x) \propto \int d\omega e^{-i\omega t + \mathbf{p}\cdot\mathbf{x}} A(\omega, \mathbf{p})$. The projectors in Eq. (1) are defined as $\tilde{\Delta}^{\mu\nu} = -\eta^{\mu\nu} + \tilde{p}^\mu \tilde{p}^\nu / m^2$ and $\tilde{\Delta}_\lambda^{(\mu} \tilde{\Delta}_\gamma^{\nu)} = \tilde{\Delta}_\lambda^{(\mu} \tilde{\Delta}_\gamma^{\nu)} - \tilde{\Delta}^{\mu\nu} \tilde{\Delta}_{\lambda\gamma} / 3$. The second line of Eq.(2) is employed a quasi-particle approximation, where the $\Delta\varepsilon_{\mathbf{p}}$ is the in-medium energy shift and is T-even. The $\Gamma_{\mathbf{p}}$ is the width of the particle, i.e. twice damping rate, of the particles in-medium, which is the T-odd and is the source of dissipation in this calculation. As shown, the α_{sh} is an odd power of $\Gamma_{\mathbf{p}}$, so it is T-odd and dissipative.

It is worth noting that terms like $\Gamma_{\mathbf{p}}/(2T)$ do not have mass suppression, allowing them to survive in non-relativistic limits. Consequently, this tensor polarization, especially the SITP effect, has a potential to be observed in low-energy physics experiments, such as plasma or cold atom systems. Meanwhile, directly extracting the in-medium mass shift and width from the shape of the invariant mass spectra of kaon pairs [43] or dileptons [44] is highly challenging. The observed spectra in experiments [28] are dominated by the spin-aligned ϕ mesons that survive to kinetic freeze-out with a vacuum spectral

function. As shown in Eq. (1) and Eq. (2), these in-medium spectral properties are naturally related to the transport coefficients generating the spin alignment, allowing us to use the spin alignment in reverse as a probe to the spectral properties of the QCD matter. In the following, we will use simple setups for the width and mass shift to study how the SITP effect manifests in phenomenology, which reversely illustrates this point.

Phenomenological setup.— We adopt the commonly used freezeout assumption for spin physics [22, 24, 45]. Specifically, we consider a physical scenario in which the ϕ meson, carrying an equilibrated spin alignment, forms as early as the late stages of the QGP [46, 47]. Depending on conditions such as centrality, beam energy, etc., the fireball evolution varies, leading the spin alignment to effectively freezeout at the QGP phase, mixed phase, or hadronic phase. This contributes to the observed centrality and beam energy dependence (see latter). After this “spin freeze-out,” the spin alignment stays approximately unchanged. The ϕ mesons surviving through the kinetic freeze-out will recover the vacuum spectral function but retain a “memory” of spin alignment from the spin freeze-out. Their decay products no longer undergo re-scattering and will carry all this information to the final observables.

We employ the standard Cooper-Fry-like formula to characterize the freezeout of spin alignment, where the $\delta\rho_{00}$ can be expressed with tensor polarization $\mathcal{T}^{\mu\nu}$ as

$$\delta\rho_{00}(\hat{n}_{\text{pr}}, \mathbf{p}) = \frac{\int d\Sigma^\lambda p_\lambda \mathcal{T}^{\mu\nu}(x, \mathbf{p}) \hat{n}_\mu(\mathbf{p}) \hat{n}_\nu(\mathbf{p})}{d\Sigma^\lambda p_\lambda 3n(\varepsilon_u)}. \quad (3)$$

The Σ^λ is the hyper-surface satisfying the freeze-out condition, and \hat{n}^μ is a shorthand for $\epsilon_{s=0}^\mu$, which is related to a three-dimensional unit vector \hat{n}_{pr} by a Lorentz boost, i.e., $\hat{n}^\mu = [\Lambda(\mathbf{p}) \cdot \hat{n}_{\text{pr}}]^\mu$, with \hat{n}_{pr} being the polarization vector $\epsilon_{s=0, \text{pr}}^\mu$ in the particle rest frame. The \hat{n}_{pr} is taken out-plane (\hat{y}) direction in this work. The hydrodynamic profile is taken from the previous work [22] using CLVisc [19] with a freeze-out temperature at 157 MeV and the AMPT initial condition [22] for Au-Au collisions at mid-centrality, where the impact parameter is around 9 fm. In the following, we will evaluate the spin alignment with α_{sh} from two setups, “physically motivated coefficients” or microscopic “quark-meson (QM) model coefficients”, aiming to extract model-independent features of SITP effects.

Physically motivated coefficients.— We first construct a physically motivated α_{sh} with the help of Eq. (2). Motivated by Ref [47–51] and the QM model discussed later, we introduce some typical momentum dependence using a Lorentz contraction $\gamma_{\mathbf{p}}^{-1} = m/\varepsilon_{\mathbf{p}} \equiv \sqrt{1 - v_{\mathbf{p}}^2}$ factor for the width and its corresponding in-medium mass shifts as $\Gamma_{\mathbf{p}} = \Gamma_0/\gamma_{\mathbf{p}}$ and $\Delta\varepsilon_{\mathbf{p}} = \Delta m/\gamma_{\mathbf{p}}$. The Γ_0 and Δm are chosen to be $\Gamma_0 = 0.1$ GeV and $\Delta m = \{-0.03, 0.01, 0.05\}$ GeV, where α_{sh} ’s for these three cases

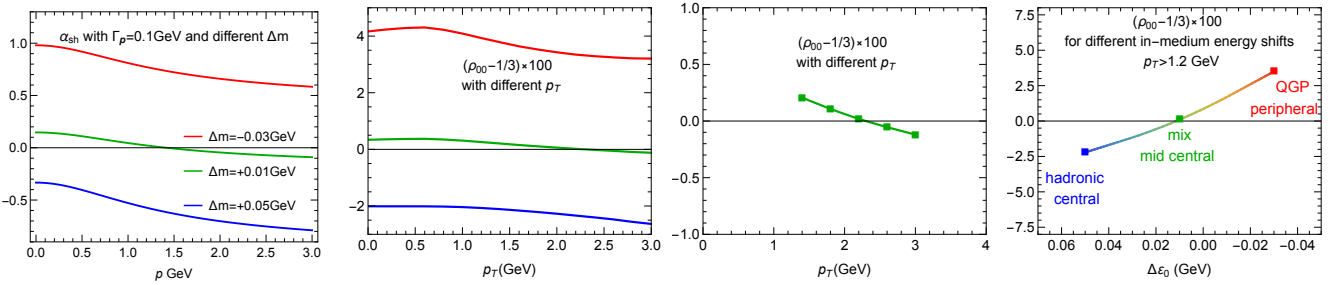


FIG. 1. (1) The α_{sh} coefficients for different cases; (2) p_T dependent ρ_{00} for three cases; (3) p_T dependent ρ_{00} for “green” coefficients in (1); (4) The p_T integrated ρ_{00} as an function of Δm .

are shown in Fig. 1. The $\Gamma_0 = 0.1$ GeV is not unreasonable large for the particles close to the phase boundary in heavy-ion collisions since even for heavy mesons like J/ψ can have a width around 0.1 GeV in this region [47, 52]. For lighter vector mesons, such as ϕ , it is reasonable to expect a width of this order. As shown, depending on the sign and magnitude of a small mass shift (ranging from -30 to 50 MeV), α_{sh} can reach values as large as “1” and as small as “ -0.8 ”. The mass shifts around the phase boundary can be huge (few hundreds MeV) [47, 53]. The sign-flipping behavior is mainly due to the competition between the $-2\Delta\epsilon_p/\Gamma_p$ and $\Gamma_p/2T$ in Eq. (2).

With these coefficients, the spin alignments ρ_{00} generated within the framework are shown in right three figures of Fig. 1. The magnitude of spin alignment ranges from -2% to the 4% , which is orders of magnitude larger than previous predictions [35] and close to what is observed in experiments [28]. Meanwhile, for all three Δm cases, the p_T dependence scales with the p dependence of the coefficients. In particular, for the $\Delta m = 0.01$ GeV case, the p_T -dependent sign-flipping behaviors observed in experiments are reproduced. Also, if the mass shifts and centrality are correlated, we can generate sign-flipping behaviors in centrality dependence (see discussions in the next section).

As a cross check of hydrodynamic calculation, we also estimate the ρ_{00} with $\mathbf{p} = 0$ in the medium rest frame using some simple math following Eq. (1):

$$\begin{aligned} \delta\rho_{00} &\propto \frac{1}{9}\alpha_{sh}\beta(\partial_z u^z + \partial_x u^x - 2\partial_y u^y) \\ \delta\rho_{00} &= \frac{1}{9}\alpha_{sh}\beta\partial_z u^z = \frac{1}{9}\alpha_{sh}\frac{\beta}{\tau}, \text{Ideal Bjorken.} \end{aligned} \quad (4)$$

With a positive α_{sh} and the fact that usually $\partial_z u^z > \partial_x u^x > \partial_y u^y$, we will get positive spin alignment. Using an ideal Bjorken hydrodynamic solution with $\alpha_{sh} \sim 1$ and $\tau \sim 6$ fm, we will have $\rho_{00} \sim 6\%$, which is not very far from the 4% obtained from a realistic hydrodynamics simulation shown in Fig. 1.

Quark-meson model coefficients.— To further justify physically motivated coefficients and obtain the model-independent insights, we have done a microscopic calculation on the coefficients and used it to calculate the

spin alignment in this section. We first evaluate the coefficients α_{sh} numerically using Eq. (2) for ϕ meson with in-medium spectral functions obtained via a 1-loop quark meson model as discussed in “supplementary materials” (similar ideas in Ref. [54]). With coupling $g_\phi = 2$, these coefficients are plotted in Fig. 2 for the cases with the effective strange quark masses $m_s = \{0.3, 0.42, 0.5\}$ GeV, which are relevant mass scales of strangeness at the QGP phase, mix phase, and hadronic phase. In the hadronic phase, this mass represents a effective in-medium kaon mass. In principle, we should switch to a purely hadronic Lagrangian, but as will be discussed later, the physics at this region is dominated by threshold effects, which are similar for both Lagrangians. Therefore, for simplicity, we delay this study to the future.

As shown in Fig. 2, microscopically calculated α_{sh} generates a p dependence and sign-flipping behaviors similar to those plotted in Fig. 1, and they share similar physics but there are some extra physics of the blue curves. For $m_s = 0.5$ GeV, which is an effective kaon mass, the ϕ meson mass is so close to the $2m_s$ threshold that Γ_p becomes much smaller, making $\Gamma_p/(2T) < 2\Delta\epsilon_p/\Gamma_p$ and α_{sh} negative for all momenta. This threshold physics will be similar if we switch to a hadronic Lagrangian with kaons [55] (with a face value of $\alpha_{sh} \sim -2$). Meanwhile, we note that the quark meson model used here does not generate large positive α_{sh} . This is because the current medium effects are dominated by radiative effects, and the effective mass shift is positive, making it difficult to generate large positive values of α_{sh} . However, in other situations where collision broadening effects dominate, large widths and negative mass shifts might occur simultaneously [47], leading to larger positive α_{sh} . Therefore, in a more realistic situation, we can expect a large positive coefficient similar to those shown in Fig. 1 in certain scenarios.

The middle two figures in Fig. 2 illustrate the p_T dependence and the “centrality dependence” of the spin alignment from the QM model. For these figures, we actually include all new effects (splitting, zeroth order) discussed in “supplementary materials” and we confirm that the SITP effect is the dominated one in this setup. The physics of the p_T dependence and the sign-flipping

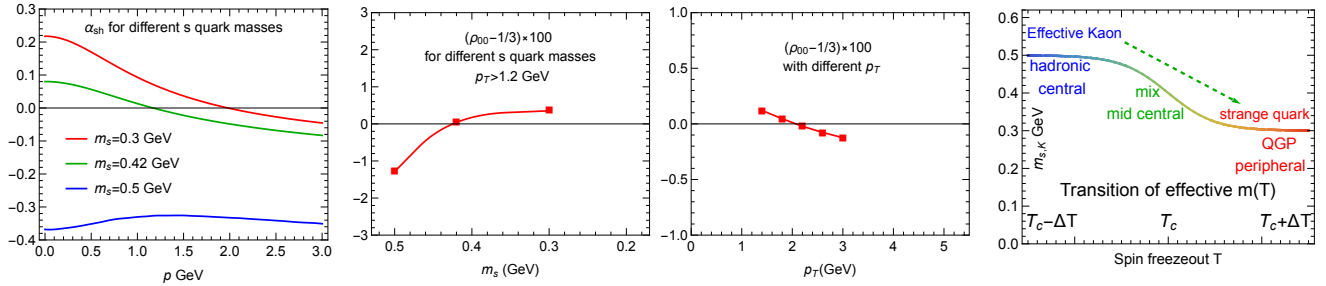


FIG. 2. (1) The α_{sh} coefficients for different cases; (2) p_T dependent ρ_{00} for “green” coefficients in (1); (3) The p_T integrated ρ_{00} as a function of m_s ; (4) illustrate how the m_s change around the phase boundary and relate to the centrality.

is the same as those discussed in Fig. 1. In this part, we will focus on discussing the “centrality dependence” as below.

The obtained m_s dependence of $\delta\rho_{00}$ could resemble the observed centrality dependence shown in Ref. [28], if we assume the mapping between m_s and centrality as: “0.5 GeV \leftrightarrow 0–20%”, “0.42 GeV \leftrightarrow 20–40%”, and “0.3 GeV \leftrightarrow 40–60%”, as illustrated in the rightmost panel of Fig. 2. Such a mapping is possible if the spin-alignments freeze out at higher temperatures for larger centralities (more peripheral), similar to the trend observed at kinetic freeze-out in Ref. [56]. This positive dependence of the freeze-out temperature on the centrality might be understandable given the centrality dependence of the fireball lifetime shown in Ref. [57]. Additionally, we also expect a shorter lifetime of the hadronic phase for more peripheral collisions [58, 59]. Colliding systems with larger centralities might be so short-lived that there is not enough time for the late-stage collisions to occur, so that the freeze-out happens earlier with higher temperatures. Meanwhile, the effective s quark mass, or the mass of alternative constituents (such as kaons in hadronic phase) of ϕ meson, might drop with temperature within a narrow ΔT window close to the QCD phase boundary, either due to chiral symmetry restoration as demonstrated in Ref. [60, 61], or due to the exhibition of the low-lying collective modes in QGP originating from non-condensate interactions as shown in Ref. [47].

Following similar physics, the collision with higher beam energy will have larger size and longer life time, so it will have a tendency to freeze out in the hadronic phase and generate a negative sign, and vice versa. This seems to explain the sign flips in the beam energy dependence of the spin alignment observed in experiments. If we further accept the $1/\tau$ enhancement of the gradient contribution in Eq. (4) at lower beam energy, it is not supersizing that we can have an increasing positive spin alignment toward lower beam energies.

On the other hand, for those who has concerns about the idea of the strange-masses-melting scenario, we can go back to the rightmost panel of Fig. 1. We just need in-medium mass shifts of ϕ changing from -30 MeV in

the QGP phase to 50 MeV (less than 10% of m_ϕ) in the hadronic phase at the phase boundary. This is not a strong requirement or unreasonable assumption. Collisional interactions in the QGP phase can generate negative mass shifts as large as few hundreds MeV [62], while radiative ($\phi \rightarrow \bar{K}K$ or $\bar{s}s$ type) interactions generate positive mass-shifts as shown in our QM model or [55]. Therefore, if the interaction type transits from collisional to radiative type as it crosses the phase boundary, we can expect a sign-flipping on mass shift, leading to sign-flipping in the spin alignment.

For other vector mesons, such as the K^* meson, we also expect significant spin alignment since the effect universally applies to all spin-1 bosons. However, due to differences in in-medium interactions, particularly during the hadronic phase, most K^* mesons observed in experiments are produced during the late hadronic phase [63]. In contrast, a much larger fraction of ϕ mesons produced in the earlier stages, can survive and be detected. Therefore, it is not supersizing that they can have different spectral properties and different spin alignment.

Summary.— We have developed a Zubarev response approach based on thermal field theory and utilized it to study the tensor polarization and spin alignment of vector mesons, leading to two key theoretical findings:

- (1) We derive for the first time a fluctuation-dissipation relation for tensor polarization and spin alignment, revealing spin alignment is naturally related to damping properties and, consequently, to the spectral functions.
- (2) We discover a novel spin-induced tensor polarization (SITP) effect at first order of hydrodynamic gradients, which can generate significant spin alignment.

There are several findings in the phenomenology study:

- (1) The SITP can lead to a spin alignment at -2% or 4%, with an in-medium width around 100 MeV and a mass shift of approximately from 50 MeV or -30 MeV.
- (2) Both physically motivated and microscopic quark-meson model calculated coefficients can produce sign-flipping behaviors of the p_T -dependent spin alignment.
- (3) Centrality-dependent spin freeze-out temperatures/spectral properties can generate sign-flipping behaviors in centrality dependent spin alignment.

This preliminary phenomenological exploration demonstrates that these newly discovered contributions can generate large spin alignment with rich behaviors, providing insights into the complex spin alignment phenomena observed in experiments. Moreover, as clearly demonstrated in the paper, spin alignment is highly sensitive to the spectral properties of particles, such as energy shifts and widths. Thus, it can potentially serve as a probe for the in-medium spectral properties of vector mesons.

In the future, we will further improve the theoretical derivation with more sophisticated microscopic calculations of the in-medium spectral properties of vector mesons, and we will also explore additional contributions beyond the leading orders [42]. Meanwhile, we need to perform quantitative phenomenological studies to directly compare the experimental data, and to accommodate non-equilibrium effects and other novel contributions proposed in Refs. [38, 41]. Additionally, the presence of the newly discovered SITP effect is robust against variations in the details of the interactions and is universal in both relativistic and non-relativistic cases. Therefore, it will be interesting to investigate this effect experimentally in low-energy physics, such as plasma physics or cold atom physics [8].

Acknowledgments We gratefully acknowledge the valuable contribution from Yi Yin, who definitely deserves a key position in the author list, but waive the authorship generously. We also especially thanks Longgang Pang who provides hydrodynamic profiles for numerical studies. We thank Hengtong Ding, Xiaojian Du, Aiqiang Guo, Koichi Hattori, Min He, Che-Ming Ko, Yutie Liang, Shu Lin, Rapp Ralf, Kaijia Sun, Subhash Singha, Shuzhe Shi, Yifeng Sun, Aihong Tang, Biaogang Wu, Dilun Yang, Wenbin Zhao, Youyu Li for valuable discussions. FL is supported by NSFC No. 12105129. SL is supported by Fundamental Research Funds for the central Universities.

* fengli@gmail.com

† Corresponding author.
lshphy@hnu.edu.cn

- [1] C. Bourrely, J. Soffer, and E. Leader, Phys. Rept. **59**, 95 (1980).
- [2] M. I. Haftel, L. Mathelitsch, and H. F. K. Zingl, Phys. Rev. C **22**, 1285 (1980).
- [3] R. J. Holt, J. R. Specht, K. Stephenson, B. Zeidman, J. S. Frank, M. J. Leitch, J. D. Moses, E. J. Stephenson, and R. M. Laszewski, Phys. Rev. Lett. **47**, 472 (1981).
- [4] M. E. Schulze *et al.*, Phys. Rev. Lett. **52**, 597 (1984).
- [5] D. Abbott *et al.* (JLAB t(20)), Phys. Rev. Lett. **84**, 5053 (2000), arXiv:nucl-ex/0001006.
- [6] K.-b. Chen, W.-h. Yang, S.-y. Wei, and Z.-t. Liang, Phys. Rev. D **94**, 034003 (2016), arXiv:1605.07790 [hep-ph].
- [7] K.-b. Chen, Z.-t. Liang, Y.-k. Song, and S.-y. Wei, Phys.

- Rev. D **102**, 034001 (2020), arXiv:2002.09890 [hep-ph].
- [8] P. D. Gregory, J. A. Blackmore, J. Aldegunde, J. M. Hutson, and S. L. Cornish, Phys. Rev. A **96**, 021402 (2017).
- [9] L. Adamczyk *et al.* (STAR), Nature **548**, 62 (2017).
- [10] J. Adam *et al.* (STAR), Phys. Rev. C **98**, 014910 (2018), arXiv:1805.04400 [nucl-ex].
- [11] T. Niida (STAR), Nucl. Phys. A **982**, 511 (2019).
- [12] J. Adam *et al.* (STAR), Phys. Rev. Lett. **123**, 132301 (2019), arXiv:1905.11917 [nucl-ex].
- [13] S. Acharya *et al.* (ALICE), Phys. Rev. Lett. **128**, 172005 (2022), arXiv:2107.11183 [nucl-ex].
- [14] Z.-T. Liang and X.-N. Wang, Phys. Rev. Lett. **94**, 102301 (2005), [Erratum: Phys. Rev. Lett. **96**, 039901 (2006)].
- [15] F. Becattini, V. Chandra, L. Del Zanna, and E. Grossi, Annals Phys. **338**, 32 (2013).
- [16] I. Karpenko and F. Becattini, Eur. Phys. J. C **77**, 213 (2017), arXiv:1610.04717 [nucl-th].
- [17] H. Li, L.-G. Pang, Q. Wang, and X.-L. Xia, Phys. Rev. C **96**, 054908 (2017), arXiv:1704.01507 [nucl-th].
- [18] Y. Sun and C. M. Ko, Phys. Rev. C **96**, 024906 (2017).
- [19] L.-G. Pang, H. Petersen, Q. Wang, and X.-N. Wang, Phys. Rev. Lett. **117**, 192301 (2016).
- [20] S. Y. F. Liu, Y. Sun, and C. M. Ko, Phys. Rev. Lett. **125**, 062301 (2020), arXiv:1910.06774 [nucl-th].
- [21] S. Y. F. Liu and Y. Yin, JHEP **07**, 188 (2021), arXiv:2103.09200 [hep-ph].
- [22] B. Fu, S. Y. F. Liu, L. Pang, H. Song, and Y. Yin, Phys. Rev. Lett. **127**, 142301 (2021), arXiv:2103.10403 [hep-ph].
- [23] F. Becattini, M. Buzzegoli, and A. Palermo, Phys. Lett. B **820**, 136519 (2021), arXiv:2103.10917 [nucl-th].
- [24] F. Becattini, M. Buzzegoli, G. Inghirami, I. Karpenko, and A. Palermo, Phys. Rev. Lett. **127**, 272302 (2021), arXiv:2103.14621 [nucl-th].
- [25] B. Fu, L. Pang, H. Song, and Y. Yin, (2022), arXiv:2201.12970 [hep-ph].
- [26] X.-Y. Wu, C. Yi, G.-Y. Qin, and S. Pu, (2022), arXiv:2204.02218 [hep-ph].
- [27] Z.-T. Liang and X.-N. Wang, Phys. Lett. B **629**, 20 (2005), arXiv:nucl-th/0411101.
- [28] M. S. Abdallah *et al.* (STAR), Nature **614**, 244 (2023), arXiv:2204.02302 [hep-ph].
- [29] B. I. Abelev *et al.* (STAR), Phys. Rev. C **77**, 061902 (2008), arXiv:0801.1729 [nucl-ex].
- [30] S. Acharya *et al.* (ALICE), Phys. Rev. Lett. **125**, 012301 (2020), arXiv:1910.14408 [nucl-ex].
- [31] S. Singha (STAR), Nucl. Phys. A **1005**, 121733 (2021), arXiv:2002.07427 [nucl-ex].
- [32] (2022), arXiv:2204.10171 [nucl-ex].
- [33] F. Becattini and F. Piccinini, Annals Phys. **323**, 2452 (2008), arXiv:0710.5694 [nucl-th].
- [34] F. Becattini, F. Piccinini, and J. Rizzo, Phys. Rev. C **77**, 024906 (2008), arXiv:0711.1253 [nucl-th].
- [35] X.-L. Xia, H. Li, X.-G. Huang, and H. Zhong Huang, Phys. Lett. B **817**, 136325 (2021), arXiv:2010.01474 [nucl-th].
- [36] F. Becattini, (2022), arXiv:2204.01144 [nucl-th].
- [37] X.-L. Sheng, L. Oliva, and Q. Wang, Phys. Rev. D **101**, 096005 (2020), arXiv:1910.13684 [nucl-th].
- [38] B. Müller and D.-L. Yang, (2021), 10.1103/PhysRevD.105.L011901, arXiv:2110.15630.
- [39] N. Weickgenannt, D. Wagner, and E. Speranza, (2022), arXiv:2204.01797 [nucl-th].

- [40] X.-L. Sheng, L. Oliva, Z.-T. Liang, Q. Wang, and X.-N. Wang, (2022), arXiv:2206.05868 [hep-ph].
- [41] X.-L. Sheng, L. Oliva, Z.-T. Liang, Q. Wang, and X.-N. Wang, Phys. Rev. Lett. **131**, 042304 (2023), arXiv:2205.15689 [nucl-th].
- [42] Y. Li and S. Y. F. Liu, (2025), arXiv:2501.17861 [nucl-th].
- [43] S. Pal, C. M. Ko, and Z.-w. Lin, Nucl. Phys. A **707**, 525 (2002), arXiv:nucl-th/0202086.
- [44] G.-Q. Li and C. M. Ko, Nucl. Phys. A **582**, 731 (1995), arXiv:nucl-th/9407016.
- [45] F. Becattini, G. Cao, and E. Speranza, Eur. Phys. J. C **79**, 741 (2019), arXiv:1905.03123 [nucl-th].
- [46] E. V. Shuryak and I. Zahed, Phys. Rev. D **70**, 054507 (2004).
- [47] S. Y. F. Liu and R. Rapp, Phys. Rev. C **97**, 034918 (2018).
- [48] R. Rapp, Phys. Rev. C **63**, 054907 (2001), arXiv:hep-ph/0010101.
- [49] H. van Hees and R. Rapp, Nucl. Phys. A **806**, 339 (2008), arXiv:0711.3444 [hep-ph].
- [50] G. Vujanovic, J. Ruppert, and C. Gale, Phys. Rev. C **80**, 044907 (2009), arXiv:0907.5385 [nucl-th].
- [51] S. Y. F. Liu and R. Rapp, Eur. Phys. J. A **56**, 44 (2020), arXiv:1612.09138 [nucl-th].
- [52] M. He, B. Wu, and R. Rapp, Phys. Rev. Lett. **128**, 162301 (2022), arXiv:2111.13528 [nucl-th].
- [53] S. Y. F. Liu and R. Rapp, J. Phys. Conf. Ser. **779**, 012034 (2017).
- [54] W.-B. Dong, Y.-L. Yin, X.-L. Sheng, S.-Z. Yang, and Q. Wang, (2023), arXiv:2311.18400 [hep-ph].
- [55] K. L. Haglin and C. Gale, Nucl. Phys. B **421**, 613 (1994), arXiv:nucl-th/9401003.
- [56] L. Adamczyk *et al.* (STAR), Phys. Rev. C **96**, 044904 (2017), arXiv:1701.07065 [nucl-ex].
- [57] B. Wu, X. Du, M. Sibila, and R. Rapp, Eur. Phys. J. A **57**, 122 (2021), [Erratum: Eur.Phys.J.A 57, 314 (2021)], arXiv:2006.09945 [nucl-th].
- [58] J. Adam *et al.* (ALICE), Phys. Rev. C **95**, 064606 (2017), arXiv:1702.00555 [nucl-ex].
- [59] S. Acharya *et al.* (ALICE), Phys. Lett. B **813**, 136030 (2021), arXiv:2007.08315 [nucl-ex].
- [60] M. Buballa, Phys. Rept. **407**, 205 (2005), arXiv:hep-ph/0402234.
- [61] F. Li, *Spinodal Instabilities in NJL and PNJL Model*, Ph.D. thesis, Texas A-M (2016).
- [62] S. Y. F. Liu and R. Rapp, *Proceedings, 47th International Symposium on Multiparticle Dynamics (ISMD2017): Tlaxcala, Tlaxcala, Mexico, September 11-15, 2017*, EPJ Web Conf. **172**, 05001 (2018).
- [63] A. Ilner, D. Cabrera, C. Markert, and E. Bratkovskaya, Phys. Rev. C **95**, 014903 (2017), arXiv:1609.02778 [hep-ph].
- [64] K. Hattori, Y. Hidaka, N. Yamamoto, and D.-L. Yang, (2020), 10.1007/jhep02(2021)001.
- [65] C. Gale and J. I. Kapusta, Nucl. Phys. B **357**, 65 (1991).
- [66] R. Rapp, G. Chanfray, and J. Wambach, Nucl. Phys. A **617**, 472 (1997), arXiv:hep-ph/9702210.
- [67] G. Baym, T. Hatsuda, and M. Strickland, Phys. Rev. C **95**, 044907 (2017), arXiv:1702.05906 [nucl-th].
- [68] E. Speranza, A. Jaiswal, and B. Friman, Phys. Lett. B **782**, 395 (2018), arXiv:1802.02479 [hep-ph].
- [69] A. Hosoya, M.-a. Sakagami, and M. Takao, Annals Phys. **154**, 229 (1984).
- [70] D. N. Zubarev, *Nonequilibrium statistical thermodynamics* (Consultants Bureau, 1974).
- [71] S. Borsanyi, Z. Fodor, C. Hoelbling, S. D. Katz, S. Krieg, and K. K. Szabo, Phys. Lett. B **730**, 99 (2014), arXiv:1309.5258 [hep-lat].
- [72] J. M. Luttinger, Phys. Rev. **135**, A1505 (1964).
- [73] G. D. Moore and K. A. Sohrabi, Phys. Rev. Lett. **106**, 122302 (2011), arXiv:1007.5333 [hep-ph].
- [74] M. Srednicki, *Quantum field theory* (Cambridge University Press, 2007).
- [75] F. J. Dyson, Phys. Rev. **75**, 1736 (1949).
- [76] J. M. Luttinger and J. C. Ward, Phys. Rev. **118**, 1417 (1960).
- [77] S. Y. F. Liu and F. Li, in preparation (2022).

SUPPLEMENTAL MATERIAL

Theoretical derivation for tensor polarization

In this section, we will provide more details on the derivation that leads to the theoretical results presented in the previous sections. We begin by introducing the *Wigner functions* of a massive vector meson with mass m and field operator V^μ :

$$\begin{aligned} W^{\mu\nu}(x, \mathbf{p}) &\equiv \varepsilon_{\mathbf{p}} \int \frac{dp^0}{2\pi} \int d^4y e^{ip \cdot y} \langle V^\mu(x_-) V^\nu(x_+) \rangle \\ &= W_+^{\mu\nu}(x, \mathbf{p}) + W_-^{\mu\nu}(x, \mathbf{p}) \end{aligned} \quad (5)$$

where $x_\pm = x \pm y/2$, $\varepsilon_{\mathbf{p}} = \sqrt{\mathbf{p}^2 + m^2}$, $\langle \dots \rangle$ denotes the thermal ensemble average, and W_\pm denote the integration over the positive and negative p^0 respectively, corresponding to the differential spin density matrix $\varrho(x, \pm \mathbf{p})$ [15], where the $\varrho(x, \mathbf{p})$ is embedded in Wigner function as

$$\begin{aligned} 2W_+^{\mu\nu}(x, \mathbf{p}) &= \sum_{s, s'} \epsilon_s^{\mu*}(\mathbf{p}) \epsilon_{s'}^\nu(\mathbf{p}) \varrho_{s's}(x, \mathbf{p}) + \delta W^{\mu\nu} \\ &\equiv \mathcal{W}^{\mu\nu}(x, \mathbf{p}) + \delta W^{\mu\nu}(x, \mathbf{p}). \end{aligned} \quad (6)$$

The factor “2” is for matching the conventional normalization of the density matrix. The $\epsilon_s(\mathbf{p})$ represents the polarization vector of the vector meson moving with momentum \mathbf{p} and occupying the spin state s , and satisfies $\tilde{p} \cdot \epsilon_s(\mathbf{p}) = 0$ with $\tilde{p} = (\varepsilon_{\mathbf{p}}, \mathbf{p})$ being the on-shell 4-momentum. So, the projected Wigner function

$$W^{\mu\nu}(x, \mathbf{p}) \equiv \sum_{s, s'} \epsilon_s^{\mu*}(\mathbf{p}) \epsilon_{s'}^\nu(\mathbf{p}) \varrho_{s's}(x, \mathbf{p}) \quad (7)$$

is perpendicular to the on-shell 4-momentum \tilde{p} as well, and can therefore be expressed as

$$\mathcal{W}^{\mu\nu}(x, \mathbf{p}) \equiv 2\tilde{\Delta}_\alpha^\mu \tilde{\Delta}_\beta^\nu W_+^{\alpha\beta}(x, \mathbf{p}) \quad (8)$$

where $\tilde{\Delta}$ is the shorthand of $\Delta(\tilde{p})$ with $\Delta^{\mu\nu}(p) \equiv -\eta^{\mu\nu} + p^\mu p^\nu / p^2$ being the projector with respect to a 4-momentum p (note $\Delta^2 = -\Delta$). The δW can always be chosen vanishing after projections. Conversely, the differential spin-density matrix can be evaluated via the projected Wigner function as (There are subtleties on this relation, but they will not affect symmetric parts of $\mathcal{W}^{\mu\nu}$ [64])

$$\varrho_{ss'}(x, \mathbf{p}) = \epsilon_{s'}^\mu(\mathbf{p}) \epsilon_s^{\nu*}(\mathbf{p}) \mathcal{W}_{\mu\nu}(x, \mathbf{p}). \quad (9)$$

The projected Wigner function can be further decomposed, according to the representation of the rotational symmetry, into three parts as

$$\mathcal{W}^{\mu\nu} = \frac{1}{3} \tilde{\Delta}^{\mu\nu} \mathcal{S} + \mathcal{W}^{[\mu\nu]} + \mathcal{T}^{\mu\nu} \quad (10)$$

where $\mathcal{S} \equiv \mathcal{W}^{\mu\nu} \tilde{\Delta}_{\mu\nu}$ is the 3D trace of $\mathcal{W}^{\mu\nu}$ and related to spin-summed phase space density, $W^{[\mu\nu]} \equiv (W^{\mu\nu} - W^{\nu\mu})/2$ corresponds to the vector polarization of the vector meson, and $\mathcal{T}^{\mu\nu}$ defined as

$$\mathcal{T}^{\mu\nu} \equiv \mathcal{W}^{\langle\mu\nu\rangle} \equiv \mathcal{W}^{(\mu\nu)} - \frac{1}{3} \tilde{\Delta}^{\mu\nu} \mathcal{S} = 2\tilde{\Delta}_\lambda^{\langle\mu} \tilde{\Delta}_\gamma^{\nu\rangle} W_+^{(\lambda\gamma)} \quad (11)$$

corresponds to the tensor polarization of the vector field, which is of the major interest in this work. Here, the round bracket “ $\langle \dots \rangle$ ” stands for symmetrizing the included space-time indices, i.e., $W^{(\mu\nu)} = (W^{\mu\nu} + W^{\nu\mu})/2$, while the angle bracket “ $\langle \dots \rangle$ ” stands for further making the tensor traceless about the included indices.

$\mathcal{T}^{\mu\nu}$ can be further expanded in terms of the hydrodynamic gradients as

$$\mathcal{T}^{\mu\nu} \approx \mathcal{T}_{(0)}^{\mu\nu} + \mathcal{T}_{(1)}^{\mu\nu} = 2\tilde{\Delta}_\lambda^{\langle\mu} \tilde{\Delta}_\gamma^{\nu\rangle} \left(W_{+(0)}^{(\lambda\gamma)} + W_{+(1)}^{(\lambda\gamma)} \right) \quad (12)$$

where the subscripts (0) and (1) stand for the zeroth and first order of the hydrodynamic gradients (or ∂). After listing all the symmetry-allowed tensor structures non-vanishing under the projection $\tilde{\Delta}_\lambda^{\langle\mu} \tilde{\Delta}_\gamma^{\nu\rangle}$ up to the order of ∂ , we further express $\mathcal{T}^{\mu\nu}$ schematically as

$$\begin{aligned} \mathcal{T}^{\mu\nu} &= \tilde{\Delta}_\lambda^{\langle\mu} \tilde{\Delta}_\gamma^{\nu\rangle} \left[\kappa_0^u u^\lambda u^\gamma + \kappa_1^u u^\lambda u^\gamma + \kappa_{\text{sh}} \sigma^{\lambda\gamma} + \kappa_T u^{(\lambda} \partial_\perp^{\gamma)} \beta \right. \\ &\quad \left. + \kappa_{\text{su}} u^{(\lambda} \sigma^{\gamma)\alpha} \tilde{p}_\alpha + \kappa_{\text{ou}} u^{(\lambda} \Omega^{\gamma)\alpha} \tilde{p}_\alpha + \dots \right], \end{aligned} \quad (13)$$

where u^μ is the flow velocity and $\beta = 1/T$ is the inverse temperature. $\partial_\perp^\mu \equiv \tilde{\Delta}^{\mu\nu} \partial_\nu$ is the transverse derivative with the flow projector $\tilde{\Delta}^{\mu\nu} \equiv \eta^{\mu\nu} - u^\mu u^\nu$. The shear stress tensor is defined as $\sigma^{\mu\nu} \equiv \partial_\perp^{(\mu} u^{\nu)} - (1/3) \tilde{\Delta}^{\mu\nu} \theta$ with bulk stress $\theta \equiv \partial \cdot u$. $\Omega^{\mu\nu} \equiv \partial_\perp^{[\mu} u^{\nu]}$ is vorticity. The SITP contribution $\kappa_{\text{sh}} \sigma^{\lambda\gamma}$ appears naturally in this symmetry analysis with a T-odd coefficient κ_{sh} that should be originated from the dissipative processes. In the following, the κ -coefficients will be evaluated near thermal equilibrium under the framework of thermal field theory and linear response theory, with inclusion of dissipative physics.

The *zeroth-order term* $\mathcal{T}_{(0)}^{\mu\nu}$ in Eq.(12) can be evaluated under exact/global thermal equilibrium and is related to the in-medium spectral function “ A ” via

$$\begin{aligned} \mathcal{T}_{(0)}^{\mu\nu} &= 2\tilde{\Delta}_\alpha^{\langle\mu} \tilde{\Delta}_\beta^{\nu\rangle} \int_0^\infty dp^0 \int d^4y e^{ip \cdot y} \langle V^\alpha(x_-) V^\beta(x_+) \rangle \\ &= 2\tilde{\Delta}_\alpha^{\langle\mu} \tilde{\Delta}_\beta^{\nu\rangle} \int_0^\infty dp^0 n(p^0) A^{\alpha\beta}(p), \end{aligned} \quad (14)$$

where $n(\omega) = 1/(e^{\beta\omega} - 1)$ is the Bose-Einstein distribution. In the thermal medium, the longitudinal and transverse modes of the vector meson are different, so that the spectral function can be decomposed as [65, 66]

$$A^{\mu\nu} = \sum_{a=L,T} \Delta_a^{\mu\nu} A_a, \quad A_a = \frac{1}{\pi} \text{Im} \frac{-1}{p^2 - m^2 - \Pi_a}. \quad (15)$$

The longitudinal and transverse projector $\Delta_{T,L}$ are $\Delta_L^{\mu\nu} = v^\mu v^\nu / (-v^2)$, $\Delta_T^{\mu\nu} = \Delta^{\mu\nu} - \Delta_L^{\mu\nu}$, where $v^\mu = \Delta^{\mu\nu} u_\nu$ is the projected flow velocity with respect to p . The on-shell version of these projectors are denoted by $\tilde{\Delta}_L^{\mu\nu} = \tilde{v}^\mu \tilde{v}^\nu / (-\tilde{v}^2)$ with $\tilde{v}^\mu = \tilde{\Delta}^{\mu\nu} u_\nu$ and $\tilde{\Delta}_T^{\mu\nu} = \Delta_T^{\mu\nu}$. Given that $\tilde{\Delta}_\lambda^\mu \tilde{\Delta}_\gamma^\nu \Delta_L^{\lambda\gamma}(p) = \tilde{\Delta}_L^{\mu\nu} (1 - \Delta\omega^2 \tilde{v}^2 / p^2)$ with $\Delta\omega = p^0 - \varepsilon_p$, we therefore obtain that

$$\mathcal{T}_{(0)}^{\mu\nu} = \alpha_0 n(\varepsilon_p) \tilde{\Delta}_L^{\langle\mu\nu\rangle} = \frac{\alpha_0}{-\tilde{v}^2} n(\varepsilon_p) \tilde{\Delta}_\lambda^\mu \tilde{\Delta}_\gamma^\nu u^\lambda u^\gamma, \quad (16)$$

$$\alpha_0 = 2\varepsilon_p \int_0^\infty d\omega \frac{n(\omega)}{n(\varepsilon_p)} \left[(A_L - A_T) - \frac{\Delta\omega^2 \tilde{v}^2}{p^2} A_L \right].$$

A_L usually has a factor proportional to p^2 cancelling with $1/p^2$ to make the integration convergent. In principle, the α_0 in Eq. (16) should be evaluated numerically using a realistic in-medium spectral function. However, if we assume a non-analytic real energy shift at zero width limit, $\alpha_0 \approx (\omega_p^T - \omega_p^L)/T$ where $\omega_p^{L/T}$ satisfying $(\omega_p^{L/T})^2 - \varepsilon_p^2 - \text{Re}\Pi_{L/T}(\omega_p^{L/T}, p) = 0$ represents the shifted dispersion relation of the longitudinal and the transverse modes, respectively.

In the medium rest frame, nonzero momentum p breaks the rotational symmetry, which results in the difference between A_L and A_T and therefore leads to the tensor polarization even in the absence of hydrodynamic gradient as expressed by the first term in α_0 in Eq. (16). Such splitting induced polarizations have also been discussed for virtual photons [67, 68], but this is the first time it has been discussed in the context vector meson in a locally equilibrated hydrodynamic medium. In addition, the projection of an off-shell in-medium particle mismatches with the on-shell final states particle, which leads to the second term in α_0 in Eq. (16).

We then turn to the *first-order term* $\mathcal{T}^{(1)}$, which is proportional to the hydrodynamic gradients and accounts for the off-equilibrium contribution induced by the system inhomogeneity.

Using the Zubarev's formalism [69, 70], we obtain a Kubo formula at vanishing chemical potential that

$$W_{+(1)}^{\mu\nu} = \varepsilon_p \lim_{\omega, q \rightarrow 0} \frac{\partial}{\partial \omega} [-\text{Im} G_{R+}^{\mu\nu\lambda\gamma}(\omega, \mathbf{q}, \mathbf{p})] \xi_{\lambda\gamma} \quad (17)$$

where the G_{R+} is embedded in retarded Green function

$$G_R^{\mu\nu\lambda\gamma}(t-t', \mathbf{x}, \mathbf{z}, \mathbf{y}) \equiv \int \frac{d\omega}{2\pi} \frac{d^3\mathbf{q}}{(2\pi)^3} \frac{d^3\mathbf{p}}{(2\pi)^3} e^{-i\omega \cdot (t-t')} \times e^{i\mathbf{q} \cdot (\mathbf{x}-\mathbf{z})} e^{i\mathbf{p} \cdot \mathbf{y}} G_R^{\mu\nu\lambda\gamma}(\omega, \mathbf{q}, \mathbf{p})$$

$$= (-i)\Theta(t-t') \langle [V^\mu(t, \mathbf{x}_-) V^\nu(t, \mathbf{x}_+), T^{\lambda\gamma}(t', \mathbf{z})] \rangle, \quad (18)$$

and $\xi_{\lambda\gamma} \equiv \beta^{-1} \partial_{(\lambda} (\beta u_{\gamma)})$. Combined with the ideal hydrodynamic equations, $\xi_{\lambda\gamma}$ can be written as a linear combination of $\sigma_{\lambda\gamma}$ and θ at the leading gradient order as

$$\xi_{\lambda\gamma} \approx \sigma_{\lambda\gamma} + \left[\frac{1}{3} \tilde{\Delta}_{\lambda\gamma} + c_s^2 u_\lambda u_\gamma \right] \theta, \quad (19)$$

where c_s^2 is the square of the sound speed, whose value at chemical freeze out, taken from lattice QCD data [71], is around 0.16. The shear part of the Kubo formula can also be obtained using metric variation in Ref [72, 73].

In Eq. (18), $T^{\mu\nu} \equiv -F^\mu_\alpha F^{\nu\alpha} + m^2 V^\mu V^\nu - \eta^{\mu\nu} (-F^2/4 + m^2 V^2/2)$ stands for the Belinfante energy-momentum tensor of the sourceless Proca field, where $F^{\mu\nu} \equiv \partial^\mu V^\nu - \partial^\nu V^\mu$. After keeping only the leading order of the skeleton expansion [74–76], we express the $G_R^{\mu\nu\lambda\gamma}(\omega, \mathbf{q}, \mathbf{p})$ in the medium rest frame as:

$$G_{R+}^{\mu\nu\lambda\gamma}(\omega, \mathbf{q}, \mathbf{p}) = - \int_0^\infty dk_0 \int_0^\infty dk'_0 \frac{n(k'_0) - n(k_0)}{\omega + k'_0 - k_0 + i0^+} \times \sum_{a,b=L,T} A_a(k) A_b(k') I_{ab}^{\mu\nu\lambda\gamma}(k, k'). \quad (20)$$

The integral limits excluding the negative energy region allow us to conveniently select out the modes that are related to the physical modes in the Wigner functions. The neglected contribution is of high orders of δ_{qp} defined later in the quasi-particle approximation schemes. With the projectors, the $I_{ab}^{\mu\nu\lambda\gamma}(k, k')$ in Eq. (20) can be explicitly written as

$$I_{ab}^{\mu\nu\lambda\gamma}(k, k') = [k^\lambda k'^\gamma + k^\gamma k'^\lambda] \Delta_a^{\nu\alpha}(k) \Delta_{b,\alpha}^\mu(k') - [k_\alpha k'^\gamma \Delta_a^{\nu\lambda}(k) \Delta_b^{\mu\alpha}(k') + k^\gamma k'_\alpha \Delta_a^{\nu\alpha}(k) \Delta_b^{\mu\lambda}(k')] - [k^\lambda k'_\alpha \Delta_a^{\nu\alpha}(k) \Delta_b^{\mu\gamma}(k') + k_\alpha k'^\lambda \Delta_a^{\nu\gamma}(k) \Delta_b^{\mu\alpha}(k')] + (k_\alpha k'^\alpha - m^2) [\Delta_a^{\nu\lambda}(k) \Delta_b^{\mu\gamma}(k') + \Delta_a^{\nu\gamma}(k) \Delta_b^{\mu\lambda}(k')] - \eta^{\gamma\lambda} [(k^\zeta k'_\zeta - m^2) \eta_{\alpha\beta} - k_\beta k'_\alpha] \Delta_a^{\nu\alpha}(k) \Delta_b^{\mu\beta}(k') \quad (21)$$

where the $k = (k_0, \mathbf{p} + \mathbf{q}/2)$, $k' = (k'_0, \mathbf{p} - \mathbf{q}/2)$.

To proceed further, we carry out the integration in the quasi-particle limit, i.e., $\Pi_{T,L}/\varepsilon_p^2 \sim \delta_{qp} \ll 1$, so that all the integral over k_0 and k'_0 can be done in the vicinity of the pole of the propagator. Also, we assume the splitting is small, i.e., $(\Pi_L - \Pi_T)/(\Pi_L + \Pi_T) \sim \delta_{sp} \ll 1$. Up to the (overall) zeroth order of δ_Γ and δ_{sp} , the off-shell contribution in the projectors in Eq.(20) can be neglected, and $\mathcal{T}_{(1)}^{\mu\nu}$ can be simplified as

$$\mathcal{T}_{(1)}^{\mu\nu} = \beta n(\varepsilon_p) \tilde{\Delta}_\lambda^\mu \tilde{\Delta}_\gamma^\nu [\alpha_{sh} \xi^{\gamma\lambda} + \alpha_{sp} \xi_p \frac{u^\lambda u^\gamma}{-\tilde{v}^2}] \quad (22)$$

where $\xi_p = (\tilde{p}^\rho \tilde{p}^\sigma) \xi_{\rho\sigma} / \varepsilon_p^2$ and

$$\alpha_{sh} = \frac{4\varepsilon_p \pi}{\beta n(\varepsilon_p)} \int_0^\infty d\omega \frac{\partial n(\omega)}{\partial \omega} (\omega^2 - \varepsilon_p^2) A_{T/L}^2(\omega, \mathbf{p}) \quad (23)$$

$$\alpha_{sp} = \frac{4\varepsilon_p \pi}{\beta n(\varepsilon_p)} \int_0^\infty d\omega \frac{\partial n(\omega)}{\partial \omega} \varepsilon_p^2 (A_T^2(\omega, \mathbf{p}) - A_L^2(\omega, \mathbf{p})).$$

Furthermore, in quasi-particle limit, the spectral function nearby the positive frequency pole can be approximately expressed as

$$A_a(\omega, \mathbf{p}) \approx \frac{1}{2\varepsilon_p} \frac{1}{\pi} \text{Im} \frac{-1}{\omega - \omega_p^a + i\Gamma_p^a/2} \quad (24)$$

where $\Gamma_{\mathbf{p}}^a = \text{Im}\Pi_a(\omega_{\mathbf{p}}^a, \mathbf{p})/\varepsilon_{\mathbf{p}}$ is the width. With an expansion of $\partial n(\omega)/\partial\omega$ to the first order of $\Delta\omega/T$ as $\propto n(\varepsilon_{\mathbf{p}})(1 - \Delta\omega/T)$, α_{sh} and α_{sp} can be further simplified as with identities $\int dx x^2 (c/((x)^2 + c^2))^2 = \pi c/2$, $\int dx (c/(x^2 + c^2))^2 = \pi/(2c)$:

$$\begin{aligned}\alpha_{\text{sh}} &\approx -\frac{2\Delta\varepsilon_{\mathbf{p}}}{\Gamma_{\mathbf{p}}} + 2\frac{\Delta\varepsilon_{\mathbf{p}}}{\Gamma_{\mathbf{p}}}\frac{\Delta\varepsilon_{\mathbf{p}}}{T} + \frac{\Gamma_{\mathbf{p}}}{2T} \sim \mathcal{O}(1) \\ \alpha_{\text{sp}} &\approx -\frac{\varepsilon_{\mathbf{p}}}{\Gamma_{\mathbf{p}}} \left(\frac{\Gamma_{\mathbf{p}}^{\Delta}}{\Gamma_{\mathbf{p}}} - \frac{\Delta\varepsilon_{\mathbf{p}}}{T} \frac{\Gamma_{\mathbf{p}}^{\Delta}}{\Gamma_{\mathbf{p}}} + \frac{\Gamma_{\mathbf{p}}}{T} \frac{\omega_{\mathbf{p}}^{\Delta}}{\Gamma_{\mathbf{p}}} \right) \sim \mathcal{O}(\delta_{\text{qp}}^{-1}\delta_{\text{sp}}).\end{aligned}\quad (25)$$

with $\Gamma_{\mathbf{p}}^{\Delta} \equiv \Gamma_{\mathbf{p}}^L - \Gamma_{\mathbf{p}}^T$ and $\omega_{\mathbf{p}}^{\Delta} \equiv \omega_{\mathbf{p}}^L - \omega_{\mathbf{p}}^T$ being the difference between the width and dispersion relations of the L and T modes. $\Delta\varepsilon_{\mathbf{p}}$ and $\Gamma_{\mathbf{p}}$ are defined as $\Delta\varepsilon_{\mathbf{p}} = \omega_{\mathbf{p}}^{L/T} - \varepsilon_{\mathbf{p}}$ and $\Gamma_{\mathbf{p}} = \Gamma_{\mathbf{p}}^{L/T}$, where the differences caused by choosing L/T are $\mathcal{O}(\delta_{\text{sp}})$. Error of the expansion is around 20%, even for relatively large $\Delta\omega/T$. For $\Gamma_{\mathbf{p}}/T(\varepsilon_{\mathbf{p}}/T) \sim 0.5$. Also, the Bose enhancement factors in Eq. (25) are neglected since $n(\varepsilon_{\mathbf{p}})$ is small for vector boson with large mass. Finally, to make the obtained α_{sh} and α_{sp} covariant, we need to replace \mathbf{p} with $p_{\perp}^{\mu} \equiv \bar{\Delta}^{\mu\nu}p_{\nu}$ and $\varepsilon_{\mathbf{p}}$ with $\varepsilon_0 \equiv \tilde{p} \cdot u$.

After comparing Eq. (16) and Eq. (22) with Eq.(13), we obtain the κ -parameters at current order as

$$\begin{aligned}\kappa_0^u &= \frac{\alpha_0}{-\tilde{v}^2} n_0, \quad \kappa_1^u = \left[\alpha_{\text{sh}} \left(c_s^2 - \frac{1}{3} \right) \theta + \frac{\alpha_{\text{sp}} \xi_p}{-\tilde{v}^2} \right] \beta n_0 \\ \kappa_{\text{sh}} &= \alpha_{\text{sh}} \beta n_0, \quad \kappa_T = 0, \quad \kappa_{\text{su}} = 0, \quad \kappa_{\text{ou}} = 0\end{aligned}\quad (26)$$

with $n_0 = n(\varepsilon_0)$. The α_0 is at least of first order in $\delta_{\text{sp}/\text{qp}}$ but of zeroth order in ∂ . Thus, \mathcal{T} in this multi-parameter expansion is at the first order of ∂ , δ_{sp} or δ_{qp} . For higher orders, there are non-vanishing contributions from $\kappa_{\text{su}} \propto \delta_{\text{sp}/\text{qp}}$ and $\kappa_T \propto$ “high order gradients”, while κ_{ou} could be nonzero with asymmetric $T^{\mu\nu}$.

Some relevant and interesting physics other than tensor polarization can be studied under the similar formalism. For example, the vector polarization for vector boson can be proven equal to 4/3 of the one for spin-1/2 particle as expected. However, due to the limited space, we would leave such discussions together with more details of the present work to our long paper [77].

More for quark-meson models

In this section, we provide some more information on the calculation of the quark meson model discussed in Sec. , where details will be included in the future works. We begin with Lagrangian of quark meson model that including only one strange quark as

$$L = \int d^4x \bar{\psi}(i\not{D} - m)\psi - \frac{1}{4}F^{\mu\nu}F_{\mu\nu} + \frac{1}{2}m^2V^{\mu}V_{\mu} \quad (27)$$

where the $D_{\mu} = \partial_{\mu} - ig_{\phi}V_{\mu}$ and $F_{\mu\nu} = \partial_{\mu}V_{\nu} - \partial_{\nu}V_{\mu}$ with V_{μ} as ϕ meson field. For this Lagrangian, with $k = q + p$, the one-loop self-energy diagram in Matsubara formalism can be expressed as

$$\Pi^{\mu\nu}(p) = -g_{\phi}^2\beta^{-1} \sum_n \int \frac{d^3\mathbf{q}}{(2\pi)^3} \text{Tr}\{\gamma^{\mu} \frac{\not{q} + m_s}{q^2 - m_s^2} \gamma^{\nu} \frac{\not{k} + m_s}{k^2 - m_s^2}\}. \quad (28)$$

Then, we proceed to sum Matsubara frequency using contour integral, take the trace and use the symmetry ($q \rightarrow -k, k \rightarrow -q$) to combine and simplify terms (details see future works). In the end, we get the medium part (subtracting the 1 from the vacuums) of the self-energy be expressed as

$$\begin{aligned}\Pi_{me}^{\mu\nu}(p) &= -4g_{\phi}^2 \int dq_0 \frac{d^3\mathbf{q}}{(2\pi)^3} (2\text{sign}(q_0)f(|q_0|))\rho_s(q_0, \mathbf{q}) \\ &\times \frac{q^{\mu}k^{\nu} + k^{\mu}q^{\nu} - g^{\mu\nu}(q \cdot k - m_s^2)}{k^2 - m_s^2}\end{aligned}\quad (29)$$

with $\rho_s(q_0, \mathbf{q}) = (\delta(q_0 - \varepsilon_{\mathbf{q}}) - \delta(q_0 + \varepsilon_{\mathbf{q}}))/(2\varepsilon_{\mathbf{q}})$, $\varepsilon_{\mathbf{q}} = \sqrt{m_s^2 + \mathbf{q}^2}$ and p understood with a $p_0 \pm i\epsilon$ for analytical continuation. The angular integral can be performed analytically, left one dimensional q integral. It is straight forward to verify $p_{\mu}\Pi_{me}^{\mu\nu} = (k_{\mu} - q_{\mu})\Pi_{me}^{\mu\nu} = 0$ from the above formula.

For the vacuum part $\Pi_{vac}^{\mu\nu} = (p^2g^{\mu\nu} - p^{\mu}p^{\nu})\pi(p)$, we just take the standard dimensional regularization part

$$\pi(p) = -8\frac{g_{\phi}^2}{(4\pi)^2} \int_0^1 dx x(1-x) \ln\left(\frac{|m_s^2 - (1-x)xm_{\phi}^2|}{m_s^2 - (1-x)xp^2}\right) \quad (30)$$

with wave function and mass counter terms δ_A and δ_m to make the numerator $(p^2(1 - \pi(p^2)) - \delta_A) - m^2 - \delta_m)^{-1}$ having the correct mass and residues.

$$\begin{aligned}\delta_A &= 8\frac{g_{\phi}^2}{(4\pi)^2} \text{PV} \int_0^1 dx \frac{x(1-x)(1-x)xm_{\phi}^2}{m_s^2 - (1-x)xm_{\phi}^2} \\ \delta_m &= -m_{\phi}^2\delta_A\end{aligned}\quad (31)$$

with PV denoted the principle value integral. For the Matsubara formalism, the above formula set is all we need to reproduce the results in [54], where the numerical results are explicitly checked and they are agree with same setup.

Backup figures for phenomenology

In this section, we present two figures that were shown in the previous version of the paper, in case the reader is interested.

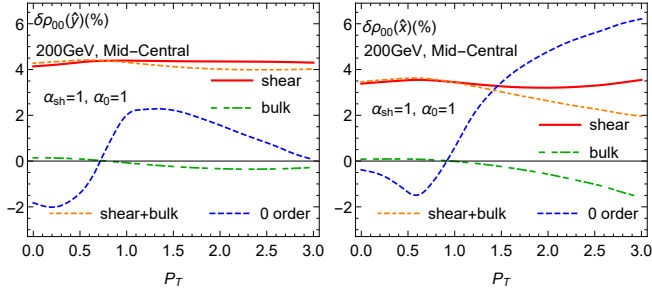


FIG. 3. The effects of the first three contributions (“0 order”, “bulk”, “shear”) in Eq. (13) with \hat{y} (left) and \hat{x} (right) as quantization axis and $\alpha_0 = \alpha_{sh} = 1$ (Using unit coefficients to highlight the effects of the flow gradients). The final results should be scaled by the physical value of α_0 and α_{sh} .

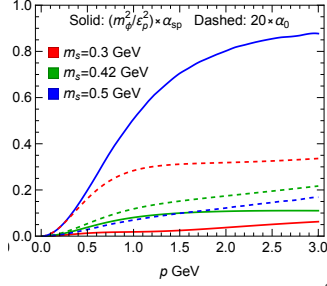


FIG. 4. Momentum dependence of the $(m_\phi^2 / \epsilon_p^2) \times \alpha_{sp}$ and $20 \times \alpha_0$ with different s quark masses for quark meson model calculations. As has been checked, the effects driven by these coefficients are sub-leading and do not affect the qualitative conclusions in the core part of the paper.